**Proceedings of ASME TURBO EXPO 2006:**
**Power for land, sea and air**
**May 9–12, 2006, Barcelona, Spain**

**GT 2006-90353**

# TECHNICAL ECONOMIC EVALUATION OF A SYSTEM FOR ELECTRICITY PRODUCTION WITH $CO_2$ CAPTURE USING A MEMBRANE REFORMER WITH PERMEATE SIDE COMBUSTION

**G. Manzolini (1)**
**Politecnico di Milano**
**giampaolo.manzolini@polimi.it**

**J.W. Dijkstra (2)**
**Energy research Centre of the Netherlands**
**dijkstra@ecn.nl**

**E. Macchi (1)**
**Full Professor of Energy Conversion (1)**
**Politecnico di Milano**
**ennio.macchi@polimi.it**

**D. Jansen (2)**
**Programme manager Clean Fossil Fuels**
**Energy research Centre of the Netherlands**
**jansen@ecn.nl**

(1) Dipartimento di Energetica, Politecnico di Milano, Piazza Leonardo da Vinci 32, 20133 Milan, Italy
(2) ECN, Energy research Centre of the Netherlands, P.O. Box 1, 1755 ZG Petten, The Netherlands

## ABSTRACT

The paper investigates the application of a novel concept, based on a membrane reactor with permeate side combustion (MRPC), to capture $CO_2$, in a natural gas fuelled power plant. The MRPC combines the steam reforming reaction on the feed side and hydrogen separation through a dense hydrogen selective membrane, with combustion of part of the permeated hydrogen, using a mixture of steam, nitrogen and air as a sweep gas. The remaining hydrogen permeated is used in the gas turbine of the combined cycle. The unconverted fuel in the high pressure $CO_2$ rich stream exiting from the membrane reactor is burned with oxygen to permit carbon dioxide sequestration.

The thermodynamic performance and economic prospects of a power plant incorporating MRPC are investigated, with a sensitivity analysis on several parameters involved. The membrane surface area required is calculated using a membrane reactor model. The final results indicate a carbon capture ratio of 100% and a net overall efficiency close to 50%. If compared to a conventional natural gas fuelled combined cycle without $CO_2$ capture, this technology leads to an increase in cost of electricity of about 30% and a $CO_2$ avoidance cost of about 30 €/t$CO_2$.

Keywords: membrane reactor, hydrogen, permeate combustion, $CO_2$ capture, system assessment.

## NOMENCLATURE AND ACRONYMS

Ea: Activation energy [J mol$^{-1}$]
T: Temperature [K]
R: Gas constant [J mol$^{-1}$ K$^{-1}$]
J: Hydrogen flux through the membrane [mol s$^{-1}$], see (7)
P: Membrane permeance [mol s$^{-1}$ m$^{-2}$Pa$^{-0.5}$], see (7)
$P_0$: Pre-exponential factor in membrane permeance equation [mol·s$^{-1}$m$^{-2}$Pa$^{-0.5}$], see (7)
$p_F$: Hydrogen partial pressure at the feed side [Pa]
$p_P$: Hydrogen partial pressure at the permeate side [Pa]
n: Exponent depending on the permeation mechanism
$\eta_{el}$: Net overall electric efficiency, see (5)
ASU: Air Separation Unit
CCR: Carbon Capture Ratio, see (6)
GT: Gas turbine
COE: Cost of electricity [€/MWh]
HRF: Hydrogen Recovery Factor, see (4)
HRSG: Heat Recovery Steam Generator
LHV: Lower Heating Value, [MJ/kg]
MRPC: Membrane Reformer with Permeate Combustion
NG: Natural Gas
S/C Steam-to-carbon ratio
TIT: First rotor total inlet temperature, [K]
VGV: Variable Guide Vanes

## INTRODUCTION

The rising world energy demand in last years has been satisfied with an increased use of fossil fuels. This has resulted in an increased concentration of carbon dioxide in the atmosphere. The possible consequences of this increase, in particular global warming, lead to the search for solutions of alternative electricity generation methods, capable of limiting $CO_2$ emissions into the atmosphere. One way is to capture the $CO_2$ associated with the use of fossil fuels and to store it in deep geological formations.

There are three main routes for capture in electricity production: (i) post combustion $CO_2$ capture; (ii) oxy-combustion and (iii) pre-combustion decarbonisation. The first category is based on chemical or physical absorption of $CO_2$ in the exhaust gases of the power plant. Amine absorption of $CO_2$ is the state-of-the-art technology. The second category consists of a close-to-stochiometric oxygen combustion. The products of the combustion are a mixture of $CO_2$ and steam. The steam can easily be separated during cooling and intercooled compression, resulting in a concentrated $CO_2$ stream available for storage. The last category is pre-combustion decarbonisation which implies transferring the energy content of methane or syngas to hydrogen; hydrogen can then be used as a fuel in a combined cycle, without any $CO_2$ emission. The standard solution for pre-combustion decarbonisation with natural gas consists of a conventional steam reformer (this can also be an autothermal reformer (ATR) or a partial oxidation reactor (POX)) and a water gas shift reactor to transfer the energy content of the natural gas into hydrogen. The $H_2/CO_2$ separation is performed (at low temperature) by physical or chemical absorption. The $H_2$ is then used in a combined cycle, while the $CO_2$ is compressed and liquefied for transport and storage. To further improve efficiency and decrease $CO_2$ avoidance costs of pre-combustion technology, schemes integrating the $H_2/CO_2$ separation and the fuel conversion steps can be introduced. This can be done by removing hydrogen during fuel conversion (steam methane reforming) with a hydrogen selective membrane, resulting in a membrane reformer. A second integration is the combustion of part of the hydrogen permeating[1]. Earlier research on integration of the reactor concept in a power cycle [2] has already indicated its attractiveness from a thermodynamic point of view.

The objective of this paper is to make a thermodynamic and economic assessment of the application of such “a membrane reformer with permeate combustion” (MRPC) in a natural gas fuelled power plant with $CO_2$ capture. Two MRPC advantages are the possibility to (i) decrease the fuel conversion temperature and (ii) increase the $H_2/CO_2$ separation temperature. Compared to the conventional solutions, both effects decrease the exergy losses.

## THE MEMBRANE REACTOR

The paper considers two options for membrane technology:

(i) The state-of-art of membrane technology, i.e. Pd/Ag (23-25% Ag in weight) membranes on a porous support [3]. Pd has the property to separate hydrogen from other gasses with a theoretically infinite selectivity. These membranes can be manufactured with a separation layer with a thickness between 3 and 5 μm [4].

(ii) proton-conducting membranes, an immature, but promising technology. Proton-conducting membranes have a higher working temperature, which is a potentially important feature for application in a membrane reactor [5]. Figure 1 illustrates the working principle of the membrane reactor.

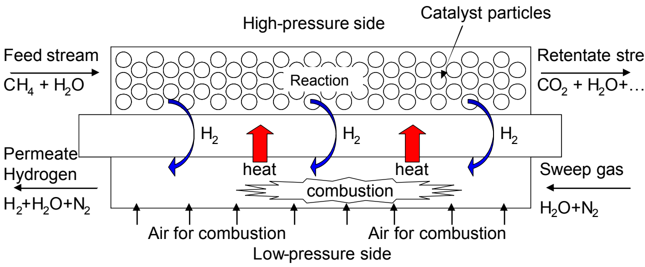

**Figure 1. Membrane reactor working principle**

At the feed side the steam methane reforming (1) and water gas shift reaction (2) take place, the combination of which leads to reaction (3):

$$\text{Steam reforming reaction: } CH_4 + H_2O \rightarrow 3\,H_2 + CO \quad (1)$$
$$\Delta H = 206.158 \text{ kJ/mol}$$
$$\text{Water gas shift reaction: } CO + H_2O \rightarrow H_2 + CO_2 \quad (2)$$
$$\Delta H = -44.447 \text{ kJ/mol}$$
$$\text{Total reaction: } CH_4 + 2H_2O \rightarrow 4\,H_2 + CO_2 \quad (3)$$
$$\Delta H = 161.711 \text{kJ/mol}$$

The total reaction is endothermic, thus a high temperature is advantageous for a high conversion. However, the selective removal of one of the products through the membrane (in this case hydrogen) allows for high conversion rates at relative low temperatures compared to conventional reforming.

A mixture of air, steam and nitrogen is used as a sweep gas and enters the reactor at the permeate side. The use of a sweep gas decreases the hydrogen partial pressure on the permeate side, thus increasing the driving force for permeation. A separate heating section is not required, since, by using air in the sweep gas mixture, part of the hydrogen is burned and the heat of combustion is used for the endothermic steam reforming reaction at the feed side. Approximately 25% of the hydrogen permeated must be burned, to satisfy the reforming reaction heat demand, and this further increases the driving force for permeation. The air is distributed along the permeate side through a perforated tube (see Fig.2). Besides air, also steam and nitrogen are used as a sweep gas, to lower the membrane surface area. This aspect is crucial at the end of the reaction zone (right side in Fig. 1), where the feed side hydrogen partial pressure is low and the airflow is limited.

The stipulated arrangement (Fig.2) for the MRPC is similar to a shell & tube heat-exchanger, whereby each tube is replaced by three concentric tubes, the external one being the membrane. The patented ECN [6] tubesheet connections to membrane is adapted. Reaction (3) takes place in the shell and hydrogen permeates through the tubular membranes. Combustion takes place inside the tubes. The feed stream enters the shell in the upper part of the reactor and leaves as retentate at the bottom. The membrane tubes are inserted in the catalyst bed and are closed-at one end to enable thermal expansion and avoid mechanical stresses. The sweep stream flows downward through the inner tube inside the membrane tube, in order to have a counter-current configuration. It requires two different separated entrances: one for air and the other for steam and nitrogen. Air must be distributed in the membrane in order to satisfy the local heat demand of reforming reaction.

For this reason, it is inserted by a perforated tube that releases the locally required amount of air for the hydrogen

---

[1] The reactor concept can also be applied for chemical synthesis [1].

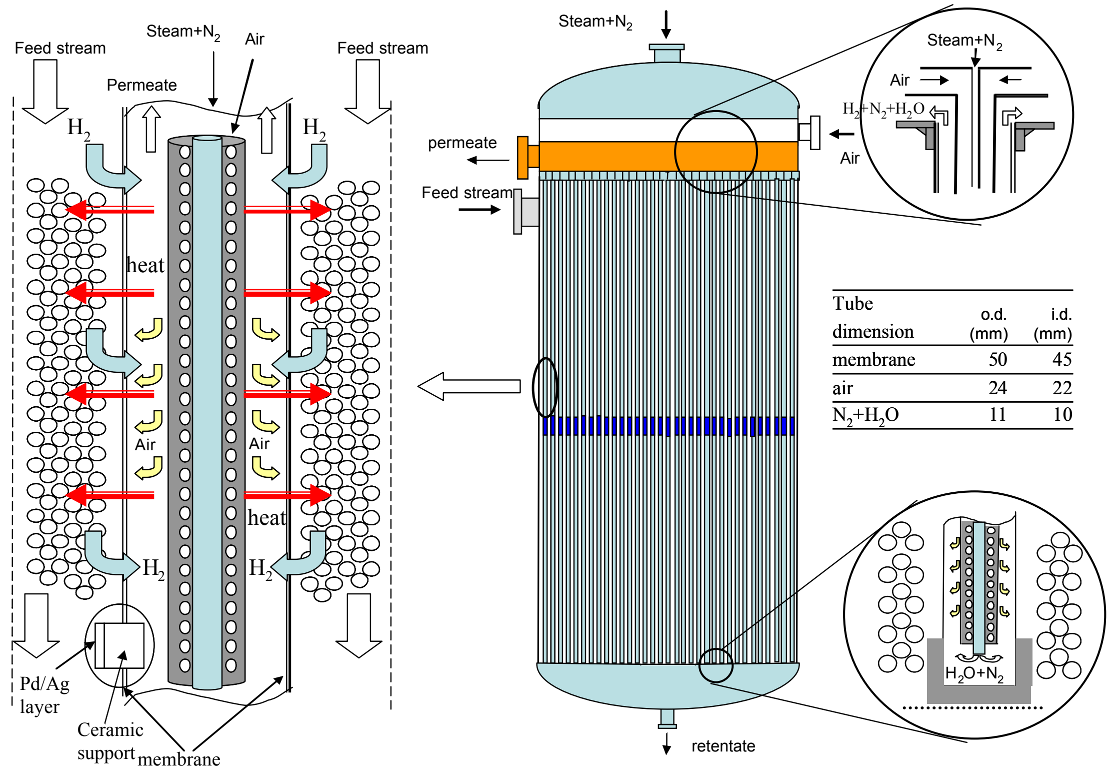

| Tube dimension | o.d. (mm) | i.d. (mm) |
|---|---|---|
| membrane | 50 | 45 |
| air | 24 | 22 |
| $N_2$+$H_2O$ | 11 | 10 |

Figure 2. Schematic of the membrane reactor design

combustion, while steam and nitrogen are inserted from the bottom at a temperature feasible with metallic materials used in advanced steam cycles.

The dimensions of the three concentric tubes used in the reactor are given in the table in Fig. 2. State-of-art technology allows manufacturing of ceramic tubes with maximum length of about 1-1.5 m. In future, this might be extended to a maximum length of 2.5 m. Increasing the length even further would give problems during manufacturing, including unfavorable temperature distribution in the ovens. To maintain a reasonable shell diameter/length ratio, an overall membrane length of 5 meter is selected, obtained by joining two tubes of 2.5 m each, by a patented sealing method [6]. The resulting overall shell dimensions are therefore about 6 m length and about 2.75 m diameter, with a membrane surface area of about 2000 $m^2$. This size is smaller than the one of the membrane reactor discussed by [7].

## SYSTEM CONFIGURATION

The base plant arrangement is presented in Fig. 3. The membrane reactor is integrated into a natural gas combined cycle. Stream 1, natural gas (NG), is pre-heated to a temperature of 250°C[2] and is then mixed with steam (2). The mixture, with a steam-to-carbon ratio (S/C ratio) of 2.95, is heated further, and enters an adiabatic pre-reformer with an exit temperature of 600°C. After pre-reforming, the stream (3) enters the membrane reactor described above. The retentate stream (4) is the stream rich in $CO_2$ and $H_2O$, with some $CH_4$, $H_2$ and CO. The latter components are combusted using $O_2$ (5), supplied by a small air separation unit (ASU), followed by an oxygen inter-cooled compressor. Burning the remaining $CH_4$ and $H_2$ is very important for system efficiency as well as for $CO_2$ stream quality. After cooling down to 35°C and water knock-out (7), the $CO_2$ stream is compressed, liquefied and pumped to the pressure of 110 bar (8), as also used in [15]. During cooling HP, IP and LP steam is produced, to be used in the HRSG of the combined cycle. The mixture of air (9), steam (10), and nitrogen (11), acting as the sweep flow, enters the reactor at the pressure dictated by the GT combustion chamber.

Steam is taken from the HRSG, air from the gas turbine compressor and then compressed by a blower to overcome the pressure drop occurring in the membrane reactor and piping, while nitrogen is taken from the ASU and compressed. The permeate stream exits the membrane reactor at a temperature of 850°C (12), required to transfer heat to the feed side. This stream is first used to heat the feed stream of the pre-reformer and then further cooled (producing HP steam) to the maximum GT combustion chamber inlet temperature (450°C) (13). The exhaust gasses from the gas turbine are cooled by a three-pressure, single re-heat, HRSG. The steam produced in the HRSG and in other parts of the system is expanded in a steam turbine. Part of the steam is extracted from the turbine at the necessary pressure and used as sweep gas in the membrane reactor.

## METHODOLOGY

### THERMODYNAMIC MODELLING METHODOLOGY

The mass and heat balances are simulated by a computer code (GS) developed to assess the performance of gas/steam cycles for power production [8-14]. The composition of all reactor products is assumed to be at chemical equilibrium.

---

[2] higher temperatures are not recommended, because of the risk of methane cracking

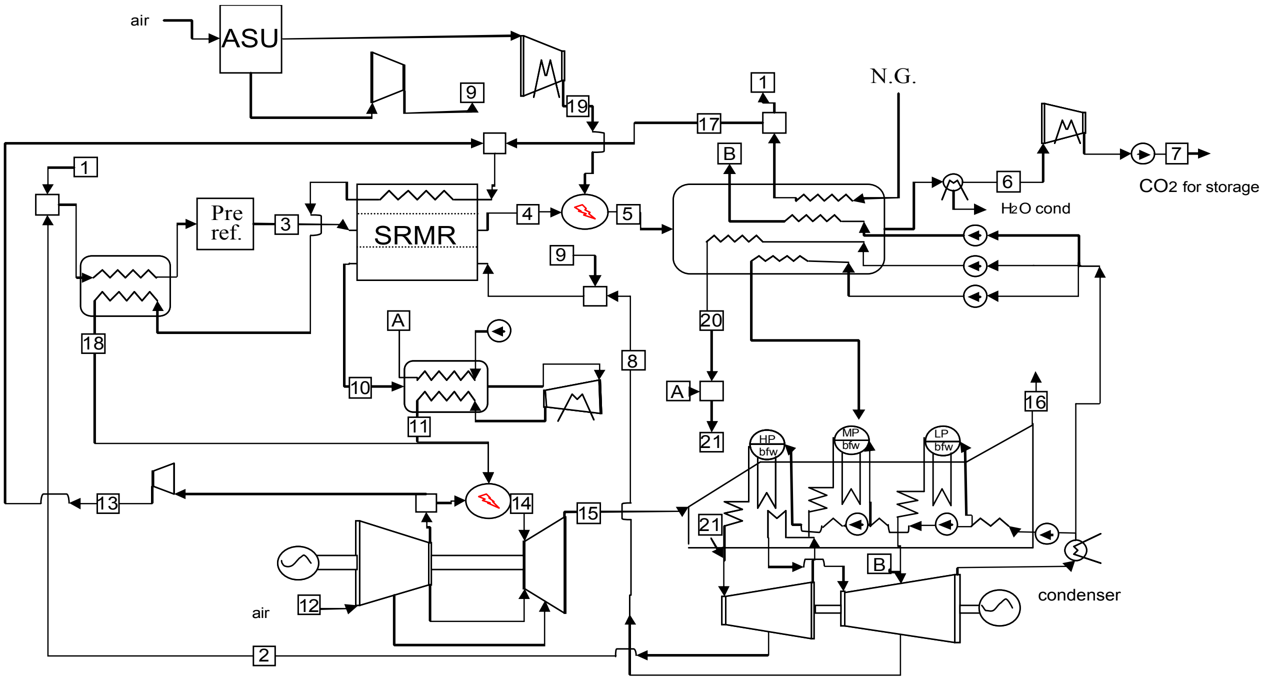

**Figure 3. Process flow diagram of the proposed power plant base on permeate combustion technology**

The $CO_2$ compressor, simulated with Aspen Plus™[3], consists of two inter-cooled stages. The NG specification is based on the pipeline quality gas from the southern part of the Norwegian off-shore reserves [15]. Oxygen is produced in a stand-alone ASU with a purity of 95% (with 1.35% $N_2$ and 3.65% of Ar) at atmospheric pressure. The ASU has been modelled as a black-box splitter with a fixed power demand of 0.261 kWh/kg$O_2$ and it's sized to produce the required oxygen.

Nitrogen used as sweep gas is 84% of total nitrogen produced, because the remaining amount is required for filters regeneration. The gas turbine model in GS is calibrated to correctly predict the performance of advanced gas turbines, accounting for all the relevant phenomena occurring like fluid-dynamic losses, cooling circuit performance, changes in gas turbine fuel and working fluid composition. The gas turbine type selected for this system is the Siemens SGT5-4000F (previous name V94.3a). A comparison between the model prediction and data of the gas turbine can be found in [16, 17].

Using hydrogen as a fuel in the gas turbine leads to higher heat transfer coefficients of the turbine working fluid. With the same turbine inlet temperature (TIT), a higher coolant flow is consequently required. At the same time, the presence of steam and nitrogen in the fuel stream decreases the amount of air needed at the inlet of the compressor to maintain a constant mass flow of the exhaust gases and to induce neglible variations in pressure ratio. For the various cases considered, the inlet air mass flow is 5% to 15% lower compared with standard conditions: it is assumed that these differences can be controlled by variable guide vanes (VGV), with negligible consequences for compressor efficiency [16]. The assumed values of the various model parameters are as follows:

| | |
|---|---|
| **Natural gas** | |
| Molar composition[4] | |
| $CH_4$ 83.9, $CO_2$ 1.8, $C_2H_6$ 9.2, $C_3H_8$ 3.3, $C_4H_{10}$ 1.4, $N_2$ 0.4 (HHV 51.463 MJ/kg, LHV 46.899 MJ/kg) | |
| Pre-heating temperature, °C | 250 |
| **Pre-reformer** | |
| Temperature inlet, °C | 680.5 |
| Temperature exit, °C | 600 |
| Pressure inlet, bar | 40 |
| Pressure loss, % | 4.0 |
| **Membrane reformer** | |
| Temperature inlet/exit, °C | 600 |
| Pressure loss, feed side, % | 10 |
| Pressure loss, permeate side, % | 1.0 |
| **Heat exchanger** | |
| Pressure loss, % | 2.0 |
| Minimum ΔT for gas-liquid heat transfer, °C | 10 |
| Pinch point ΔT for evaporators, °C | 8.0 |
| Heat losses, % of heat transferred | 0.7 |
| **ASU and oxygen compressor** | |
| $O_2$ purity, % vol | 95 |
| Power consumption, $kWh_{el}$/kg of pure $O_2$ | 0.261 |
| Pressure of $O_2$ and $N_2$ delivered by ASU, bar | 1.05 |
| $O_2$ compressor isentropic efficiency, % | 82 |
| **Gas turbine (Siemens SGT5-4000F)** | |
| Turbine inlet temperature, °C | 1350 |
| Combustor inlet pressure, bar | 17.06 |
| Combustor pressure drop, % | 3.0 |
| Exhaust mass flow, kg/s | 644.0 |
| **$CO_2$ compression** | |
| Final delivery pressure, bar | 110 |

---

[3] This code accounts for real gas effects, while GS is based on pure ideal gases, steam, or steam/gas mixtures.

[4] Desulphurization can be done with a ZnO absorption bed, with no significant influence in the overall performance and economic results

| | |
|---|---|
| Compressor isentropic efficiency, % | 82 |
| Temperature for $CO_2$ liquefaction, °C | 25 |
| Pressure drop for intercooler and dryer, % | 1.0 |
| Pump efficiency, % | 75 |
| **Steam cycle** | |
| Steam evaporation pressures, bar | 166,36,4 |
| SH and RH temperature, °C | 565 |
| Condensation pressure, bar | 0.05 |
| Pinch point $\Delta T$, °C | 8 |
| Minimum $\Delta T$ in SH and RH, °C | 25 |
| **Electrical & Auxiliaries, %** | |
| Generator efficiency, % | 98.7 |
| Gas turbine package, % of GT gross power | 0.2 |
| Steam cycle, % of rejected thermal power | 1.0 |
| Balance of plant, % of net power output | 0.15 |
| **Membrane Permeance** | |
| Pd/Ag membrane, $mol s^{-1} m^{-2} Pa^{-0.5}$ | $9.68 \times 10^{-3}$ |
| Proton-conducting membrane, $mol s^{-1} m^{-2}$ | $1.13 \times 10^{-2}$ |

In principle, using hydrogen as fuel would lead to high $NO_x$ formation, due to the high adiabatic flame temperature, as well as the use of diffusion burners (the fuel stream cannot be premixed with air). However, the combustion temperature in membrane reactor is between 850-950°C, so there should not be any problem of $NO_x$ formation. In the gas turbine combustion chamber the hydrogen is already diluted with sweep gas and $H_2O$ from the $H_2$ combustion in the membrane reactor. The final adiabatic flame temperature is about 2000 K, much lower than limits usually assumed to prevent $NO_x$ formation [16]. Two important parameters that significantly affect the system performance are hydrogen temperature and pressure at the inlet of the gas turbine combustor. Values assumed are 450°C as in [16] and a 15% pressure increase with respect to combustor pressure. A further increase of the hydrogen pressure would lead to low difference in overall efficiency, but would largely penalise the membrane surface requirement.

The parameter HRF (Hydrogen Recovery Factor) defines the ratio between hydrogen permeated and the maximum hydrogen that can be removed from the system, taking into account hydrogen formation in the reactor using the steam reforming/water gas shift reaction:

$$HRF = \frac{separated \;\; H_2}{max \;\; amount \;\; H_2} = \frac{H_2}{H_2 + CO + 3 \cdot CH_4} \qquad (4)$$

The results of the thermodynamic simulations are expressed in terms of the (net electrical LHV) efficiency and the $CO_2$ capture ratio, given respectively by:

$$\eta_{el} = \frac{Net \;\; Power}{Thermal \;\; Power \;\; Input \;\; (LHV_{NG})} \qquad (5)$$

$$CCR = \frac{CO_2\, captured}{max amount CO_2 produced from fuel used} \qquad (6)$$

MEMBRANE REACTOR MODELING METHODOLOGY

The membrane reactor surface area is the key parameter affecting the membrane reactor costs. Therefore, a one–dimensional steady state model was developed to accurately predict the membrane surface area. The model consists of ordinary differential equations describing the mass balances along the membrane length. The model incorporates:

- The kinetics of the water gas shift and steam reforming reaction on the feed side
- Permeation of individual components along the membrane length, with different permeation models available.

The model assumes constant temperature at each side of the membrane and ideal gas behaviour. Infinitely fast combustion of all hydrogen permeated occurs at the permeate side. The distribution of air along the membrane surface area has been simulated by describing the membrane reactor with 10 of the above described models (nodes) connected in a countercurrent flow configuration. Air is evenly distributed between the 10 nodes of the model. Variations of the membrane surface area have been performed with a single node model applying a correction factor between the 10 node and the 1 node model.

The permeation rate of hydrogen through the Pd/Ag membrane J (mol/s) is expressed by:

$$J = P\left(p_F^n - p_P^n\right) = P_0 \cdot e^{-\frac{Ea}{RT}}\left(p_F^n - p_P^n\right) \qquad (7)$$

where P is the permeance (mol $s^{-1} m^{-2} Pa^{-n}$) of the membrane, $p_F$ and $p_P$ partial pressures of $H_2$ on the feed and permeate side of the membrane respectively (Pa). The exponent n is related to the rate determining step in permeation through the membrane. Permeance is a function of the temperature as shown in (7). The parameters used for the simulations with Pd/Ag membranes are: n=0.5, Po=0.2161 mol $s^{-1}$ $m^{-2}$ $Pa^{-0.5}$ and Ea=22.5 kJ/mol. Infinite $H_2$ selectivity has been assumed.

It is clear from (7) that a high temperature is beneficial for the permeance (i.e. permeance goes from 1.9 mol·$s^{-1} m^{-2} Pa^{-0.5}$ at 300°C to 9.7 mol $s^{-1}$ $m^{-2} Pa^{-0.5}$ at 600°C). Maximum working temperature for this type of membrane is 650 °C [18]. The value of the permeance chosen to calculate the membrane surface area is based on [4], but a 50% reduction was assumed to take into account the permeance decrease due to operation using a syngas mixture instead of only hydrogen as a feed gas[5]. For cases with membrane temperature higher than 650°C, proton-conducting type membranes will be used. For proton-conducting membrane, which permeation law is different from formula (7) and, as immature technology, with few experimental results, a constant value of permeance equal to $1.13 \cdot 10^{-2}$ mol $m^{-2}$ $s^{-1}$ as reported in [5] was assumed. The analysis of the permeate combustion requires a detailed simulation of heat exchange in the reactor, to find (i) the limit feed temperature for Pd/Ag membrane application and (ii) the temperature required at the permeate side to satisfy the heat demand of the reforming reaction. This investigation focuses on the radial heat transfer from the permeate side to the centre of the feed side, where the reforming reaction takes place.[6] The heat transfer in the membrane reactor has been studied according to [19]. The model describes heat transfer from the permeate side through the wall and catalyst bed. The results show that the heat conductivity coefficient in the fixed bed is very low (about 2.5 W $m^{-1} K^{-1}$), with a low dependence on the bed porosity and catalyst diame-

---

[5] Reduction based on ECN experiments

[6] Axial heat transfer is considered much less important.

ter. The overall heat transfer coefficient calculated from the permeate side to the catalyst bed is about 40 W/m$^2$K. The temperature distribution in the reactor is determined by the temperature of the feed stream and the total heat required by reforming reaction. Temperature range analysed is between 600 and 650°C.

The radial temperature distribution in reactor is reported in Fig. 4. These results indicate that, while it is possible to use a Pd/Ag membrane for a reforming temperature below about 615°C, (considering a small safety margin will be used up to a feed temperature of 600°C) proton-conducting membranes are required for higher temperatures. Furthermore the results indicate that a permeate side outlet temperature of 850°C is required for ensure adequate heat transfer.

To gain additional confidence in the reactor performance it is advised to conduct a more detailed study which does not only describe heat transfer but also considers reaction kinetics, mass transfer and permeation, and also the interaction between these phenomena. This study could give more insight in optimal reactor operational and design parameters and could address issues as avoiding hot-spots.

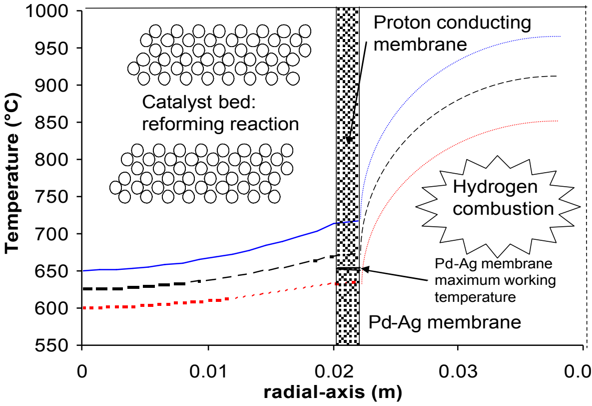

**Figure 4. Temperature profile in the membrane reactor for different feed temperatures**

ECONOMIC ASSESSMENT METHODOLOGY

The aim of the economic assessment is to make an estimation of the final cost of electricity (COE), and compare the proposed solution with conventional solutions from economic point of view. For this analysis, the method used in IEA studies [15, 20] was applied: according to the predicted investment cost, the COE is calculated by setting the net present value (NPV) of the power plant to zero. This can be achieved by varying the kWh price until the revenues balance the cost over the whole life time of power plant.

The main assumptions are reported in table 1 (the NG price is increased with 100% compared to IEA assumptions, following recent NG price developments). As in the IEA calculations, the combined cycle is composed of two gas turbines and one steam turbine. The investment cost of the main plant components are calculated as indicated in table 2. Data are mostly taken from [21], while the investment cost of the pre-reformer and membrane reactor are calculated as follows.

**Table 1. Main economic assumptions**

| | | |
|---|---|---|
| Load factor | 85 | % |
| Natural gas price | 5 | €/GJ |
| Operating lifetime | 25 | Year |
| Membrane and catalyst lifetime | 3 | Year |
| Discount rate | 10 | % |
| Maintenance (% installed plant costs) | 2.5 | %/y |
| Insurance (% installed plant costs) | 2 | %/y |
| Labour cost | 3.22 | M€/y |
| Currency conversion, $/€ | 1.25 | |
| Cost for $CO_2$ transport and storage | N/A | |

The pre-reformer catalyst volume is calculated using the space velocity and then corrected for the advancement of the reaction. The volume of the reactor considered is assumed to be twice the catalyst volume. Table 3 summarises the main assumptions for pre-reformer cost prediction. The calculation of the membrane reactor cost is complicated by its complex mechanical arrangement, for which no analogies are available. For this reason, an estimation method has been developed, based on the

**Table 2. Summary of the cost calculation starting points for each component**

The total cost, C, of a component having Scaling parameter S, is related to the reference cost $C_o$ by the relationship $C=C_o(S/S_o)^f$

| Component | Scaling parameter | Ref Size Value | Ref cost (M€) | f |
|---|---|---|---|---|
| Pre-reformer | NG input ($MW_{LHV}$) | 1800 $MW_{th}$ | 17.50 | 0.75 |
| Membrane reactor | N° of modules | 1 | 14.54 | 1 |
| Nitrogen compressor | Power | 10 MW | 3.76 | 0.67 |
| ASU | Oxygen produced | 1839.0 tonn$O_2$/d | 40.4 | 0.5 |
| Oxygen compressor | Power | 10 MW | 5.04 | 0.67 |
| Heat exchanger + HRSG | Heat exchange surface area | 225,000 m$^2$ | 54.8 | 0.67 |
| Blower | Power | 1 MW | 0.23 | 0.67 |
| $CO_2$ compression | Power | 13 MW | 18.43 | 0.67 |
| Gas turbine | Output power | 266 MW | 58.24 | 0.3[1] |
| Condenser + steam turbine | S.T. gross power | 136 MW | 47.36 | 0.67 |

[1] This exponent is low because turbomachines are the same but, due to the different fuel and power, combustor and electric generator will be different.

stipulated design, using conservative assumptions. As introduced earlier, the membrane surface required by the power plant is satisfied using multiple membrane modules of about 2000 $m^2$ each. The price of a conventional AISI 316L heat exchanger [22] is taken as a starting point for the membrane reactor costs. Based on this, the cost of reactor shell is calculated applying conservative correction factors for materials, pressure, and additional manifolding.

**Table 3. Cost calculation for pre-reformer (1800 $MW_{th}$ natural gas feed)**

| | | | M€ |
|---|---|---|---|
| Reactor | $C_0$ | | 2.75 |
| Catalyst | $C_1$ | 800 (€/$dm^3$)[7] | 6.81 |
| Insulation | $C_2$ | 1000 (€/$m^2$) | 0.04 |
| Bought out cost | $C_3$ | $(C_0 + C_1 + C_2)$ | 9.60 |
| Piping, instrumentation, installation etc. | $C_4$ | $C_0 \times 110\%$ | 3.17 |
| Contingency costs | $C_5$ | $C_3 \times 37\%$ | 4.73 |
| Installed costs | $C_{inst}$ | $(C_3 + C_4 + C_5)$ | 17.50 |

Hereon additional costs for membranes, sweep tubes and catalyst are added to provide the membrane module costs. The assumptions used to calculate total installed membrane reactor cost are summarized in table 4. The additional costs for the installed costs are calculated excluding cost of membranes and catalyst. In the case with 64 bar as feed pressure, a multiplication factor of 1.25 is adopted for the shell cost.

**Table 4. Cost calculation for membrane reactor (single module of 2000 $m^2$ membrane surface area)**

| | | | M€ |
|---|---|---|---|
| Reactor shell | $C_0$ | | 2.16 |
| Catalyst | $C_1$ | 800 (€/$dm^3$) | 3.39 |
| Insulation | $C_2$ | 1000 (€/$m^2$) | 0.07 |
| Membrane | $C_3$ | 1500 (€/$m^2$) | 3.00 |
| Sweep tubes | $C_4$ | 241 ( €/$m^2$) | 0.35 |
| Bought out cost | $C_5$ | $C_0 + C_1 + C_2 + C_3 + C_4$ | 8.96 |
| Piping, instrumentation, installation etc. | $C_6$ | $C_0 \times 110\%$ | 2.46 |
| Contingency costs | $C_7$ | $(C_5 + C_6 - C_3)*37\%$ | 3.12 |
| Installed costs | $C_8$ | $C_5 + C_6 + C_7$ | 14.54 |

## RESULTS AND DISCUSSION

The system performance, both energy- and cost-wise, are influenced by several parameters involved in the design, including:

- Membrane surface area
- S/C ratio at the inlet of the reactor
- HRF
- Feed side pressure
- Reactor temperature
- Temperature of the hydrogen at the inlet of the combustor.

Before presenting the detail of results obtained, let's briefly discuss the influence of these parameters separately:

- Membrane surface area: as it could be easily predicted, the larger the membrane surface, the better the efficiency. An economic analysis will determine the best trade-off between efficiency and investment costs. Figure 5 depicts the efficiency and the COE variation versus membrane surface area[8]. The different membrane surface areas are obtained by varying the steam mass flow rate in the sweep gas mixture. The optimum value for the COE is found for membrane area of around 14,000 $m^2$ (7 modules).
- S/C ratio has a large effect on the system efficiency: except from aspects regarding reactions kinetics and carbon formation, it would be better to work with the lowest S/C ratio as possible. In this work, a conservative value of 2.95 will be assumed. For a comparison, the optimal case was studied also with an S/C ratio of 2.75.
- HRF: some preliminary optimisations were performed in order to evaluate the influence of this parameter (Fig. 6). As shown in the figure, the HRF influences both the net electrical efficiency and the COE. While in terms of efficiency it would be better to adopt values for HRF as large as possible, an optimum value exists in term of COE: when this value is exceeded, the cost saving related to lower NG specific consumption is offset by increase in term of investment costs. On the basis of these preliminary calculations, a constant value for HRF of 95% was assumed.
- Feed side pressure: increasing pressure, increases the hydrogen partial pressure at the feed side, thus a lower amount of sweep gas and/or membrane surface area required. However, natural gas compression is required. In this study, a value of 40 bar (equal to the natural gas supply pressure) was selected as the base case. Some cases with higher (64 bar) value are also analyzed.
- Reactor temperature: in principle, increasing the temperature has a positive influence on plant performance, but it requires an increase of the inlet temperature of the combustor as well. Also, above 600 °C, it is necessary to substitute Pd/Ag supported membranes with the proton conducting type, with a corresponding decrease in permeance. The increased concentration of hydrogen due to temperature cannot compensate for the lower permeance of proton-conducting membranes compared with Pd/Ag, so the membrane surface required will be larger. Probably, this solution will be interesting only if proton-conducting membrane can reach a permeance close to that of Pd/Ag membranes, or if their price will pay off the different permeance.
- Hydrogen temperature at the combustor inlet: increasing the temperature of the fuel at the inlet of the combustor always decreases exergy losses due to combustion. In this study a temperature of the fuel of 450°C is assumed as technological limit as in [16]. Increasing this temperature with 100°C will lead to an efficiency gain of 0.4%. Decreasing this temperature to 350°C, will lead to an efficiency drop by 0.4%.

---

[7] At the membrane reactor conditions normal nickel based reforming catalyst are not suitable. Very expensive noble-metal catalyst is required.

[8] The different membrane surface areas are obtained by varying the steam mass flow rate in the sweep gas mixture.

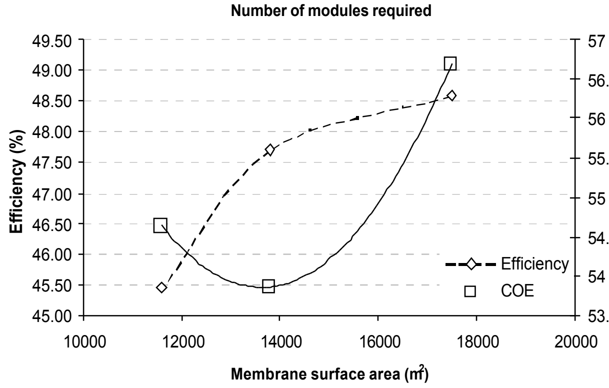

Figure 5. Efficiency and COE for different membrane surface areas for HRF of 95%

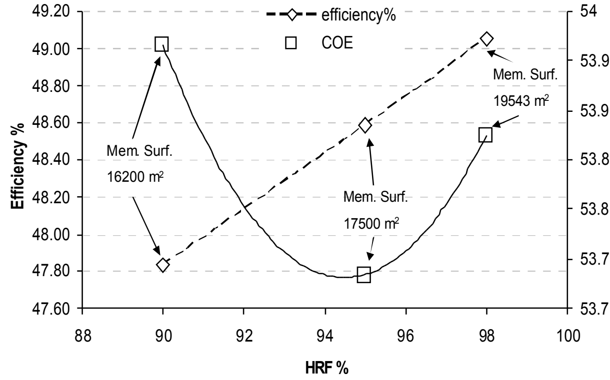

Figure 6. Efficiency and COE calculated for different HRF

Table 6 presents, both in terms of energy balances and economic parameters, the results for all the cases while the properties of the most important streams for the B2 base case are reported in table 5: (i) three base cases with varying membrane surface area (B1, B2, B3); (ii) two cases with a higher membrane reactor temperature using proton-conducting membranes (PC650, PC700), and (iii) two cases with a higher feed pressure and variation of S/C ratio (B64, O64). For comparison, the last two columns give values referring to a conventional NG combined cycle (based upon the same GTs) without capture and with post combustion capture using amine absorption (MEA) as used in [15]. All cases but one (B3) have a higher efficiency than conventional post combustion capture technology. This is a good result, also because permeate combustion option leads to a carbon capture ratio of 100%, compared to 85% of conventional technology.

For the costs analysis, the overall investment costs can be subdivided into three blocks: power section, hydrogen production and $CO_2$ capture, as reported in Tab. 5. Both the membrane and the catalyst replacement costs play a significant role in the COE. The ratio between the total invested capital and the Bought out cost is 2.1. This value is lower than usually experienced in power plant because membrane and catalyst have a significant contribution to the costs and don't affect piping, instrumentation, etc.. Looking at base cases (first three columns), as anticipated, there is a trade-off between the higher specific investment costs related to large membrane surface areas and the lower variable costs related to higher efficiency. This trade-off indicates case B2 as the one with lower COE (see also Fig. 5). Opposite to post-combustion capture, permeate combustion technology increases the ratio between power generated by the gas turbine and steam turbine. This has a positive effect on overall investment costs, because specific costs related to the gas turbine are much lower than the steam cycle costs. Compared to conventional NGCC without $CO_2$ capture, this solution increases COE of 33%; this difference is mainly related to the cost of the membrane reactor and efficiency penalties. Compared to conventional post combustion capture, case B2 has a slight decrease in COE of 2%, but yields $CO_2$ avoidance costs that are 25% lower. As expected, proton-conducting membranes are not a competitive technology, due to the high membrane investment costs related to the low permeance of this type of membrane assumed. Increasing feed pressure and decreasing S/C ratio, the case "O64" reported in table 6, leads better efficiency as well as lower investment costs, with consequently lower COE, compared to B2.

This case has a COE of 51.81 €/MWh and cost of $CO_2$ avoidance costs of 31.2 €/t$CO_2$. $CO_2$ avoidance costs are about 36% of conventional technology thanks to higher electrical efficiency and carbon capture ratio and lower specific investment cost of this solution. A sensitivity analysis on pre-reformer and membrane reactor cost has been done, to investigate the effect of our conservative assumptions on the COE. The results are shown Fig. 7, with costs lowered by 33% and increased by 50%.

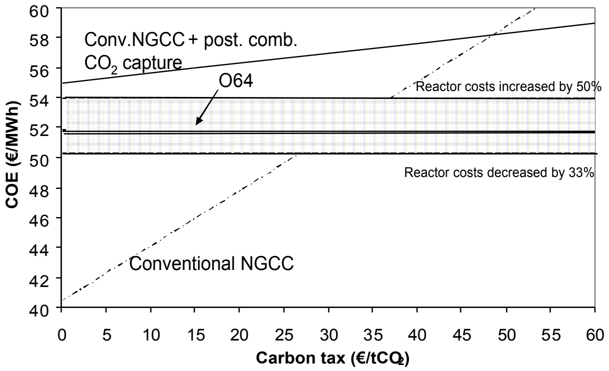

Figure 7. Carbon tax calculation with a sensitivity analysis on reactor (pre-reformer and membrane reactor) costs.[9]

As shown in the figure, even with reactor cost increased by 50%, permeate combustion is still cheaper than conventional post combustion technology. Decreasing the costs by 33%, will lower COE of about 2.5% with a carbon tax required to produce electricity cheaper than NGCC without $CO_2$ capture of about 27 €/t$CO_2$. As already stated, economic assumptions chosen are believed to be quite conservative and do not consider scale-up due to widespread industrial production.

---

[9] COE calculated without considering $CO_2$ transport and storage costs. This value would rise of 0.8 €/t$CO_2$ applying a $CO_2$ transport and storage of 4 €/t$CO_2$as in [21]

**Table 5. Summary of thermodynamic and economic results, together with reference cases**

| | Base case | | | Proton-conducting membrane | | Feed 64 bar | | NGCC | NGCC+ Post comb capture |
|---|---|---|---|---|---|---|---|---|---|
| | **B1** | **B2** | **B3** | **PC650** | **PC700** | **B64** | **O64** | | |
| Feed temperature (°C) | 600 | 600 | 600 | 650 | 700 | 600 | 600 | | |
| Feed pressure (bar) | 40 | 40 | 40 | 40 | 40 | 64 | 64 | | |
| HRF (%) | 95 | 95 | 95 | 95 | 95 | 95 | 95 | | |
| S-C ratio | 2.95 | 2.95 | 2.95 | 2.95 | 2.95 | 2.95 | 2.75 | | |
| Membrane surface area $10^4 m^2$ | 1.8 | 1.4 | 1.2 | 11 | 6.8 | 1.0 | 1.0 | | |
| Gas turbine (MW) | 666.0 | 696.3 | 731.6 | 659.8 | 653.5 | 663.7 | 663.2 | 511.7 | 725.0 |
| Steam cycle (MW) | 207.8 | 197.2 | 184.6 | 232.1 | 252.3 | 215.1 | 221.0 | 258.1 | |
| $CO_2$ clean-up & compression (MW) | 7.6 | 7.9 | 8.3 | 7.7 | 7.8 | 3.6 | 3.6 | | 30.0 |
| BOP auxiliaries (MW) | 18.9 | 19.9 | 21.1 | 19.5 | 20.1 | 26.5 | 26.5 | | 33.0 |
| Net Power (MW) | 839.6 | 857.8 | 878.4 | 857.0 | 870.2 | 845.2 | 850.5 | 769.9 | 662.0 |
| Thermal power input (MW) (referred to $CH_4$ LHV) | 1728.2 | 1790.6 | 1932.5 | 1756.4 | 1784.7 | 1738.4 | 1740.7 | 1354.4 | 1396.0 |
| **Net electrical efficiency (%)** | **48.58** | **47.90** | **45.45** | **48.79** | **48.76** | **48.62** | **48.86** | **56.84** | **47.42** |
| **Carbon Capture Ratio (%)** | **100** | **100** | **100** | **100** | **100** | **100** | **100** | **N/A** | **85.14** |
| Electricity production, (MWh/y)[a] | 6.25 | 6.39 | 6.54 | 6.38 | 6.48 | 6.29 | 6.33 | 5.73 | 4.93 |
| Gas consumption, $(GNm^3/y)$[a] | 1.11 | 1.15 | 1.21 | 1.12 | 1.14 | 1.11 | 1.11 | 0.87 | 0.89 |
| Investment Costs | | | | | | | | | |
| Combined cycle[1], (M€) | 350.1 | 351.7 | 355.3 | 354.1 | 357.3 | 367.3 | 366.6 | 283.4 | 310.6 |
| Hydrogen production[2], (M€) | 159.3 | 130.5 | 110.4 | 821.3 | 523.0 | 113.9 | 114.2 | | |
| $CO_2$ clean-up & compression[3], (M€) | 14.1 | 14.5 | 14.9 | 14.2 | 14.4 | 11.0 | 11.0 | | 149.5[b] |
| **Total Investment costs, (M€)** | **523.6** | **496.7** | **485.2** | **1189.7** | **894.7** | **492.2** | **491.8** | **283.4** | **460.1** |
| Specific Investment costs, $(€/kW_{inst})$ | 623.6 | 579.0 | 552.4 | 1388.2 | 1028.2 | 582.3 | 578.2 | 368.1 | 695.0 |
| Operation and Maintenance Costs | | | | | | | | | |
| Average capital cost, (M€/y) | 77.6 | 73.6 | 71.9 | 176.2 | 132.5 | 72.9 | 72.8 | 42.0 | 68.1 |
| Fixed cost (M€/y) | 13.7 | 13.2 | 12.8 | 27.0 | 21.1 | 13.1 | 13.1 | 8.9 | 12.4 |
| Variable cost (M€/y)[a] | 242.2 | 251.1 | 268.9 | 230.7 | 251.3 | 242.1 | 235.9 | 257.1 | 256.0 |
| Membrane substitution[4], (M€/y) | 8.8 | 6.9 | 5.8 | 53.1 | 33.5 | 5.1 | 5.1 | | |
| Catalyst substitution[4], (M€/y) | 10.2 | 8.0 | 6.7 | 61.7 | 38.9 | 5.9 | 6.0 | | |
| **Cost of electricity, (€/MWh)** | **56.70** | **53.86** | **54.64** | **81.75** | **68.75** | **52.09** | **51.81** | **40.42** | **54.92** |
| **$CO_2$ avoidance costs, (€/t$CO_2$)** | **44.55** | **36.79** | **38.92** | **113.10** | **77.52** | **31.93** | **31.17** | **N/A** | **48.55** |

[a] refers to 85% load factor

[b] 78% depends on $CO_2$ absorption and the remaining on $CO_2$ compression

[1] gas turbine and heat recovery steam cycle

[2] prereformer, membrane reformer and nitrogen compressor

[3] $CO_2$ compressor/pump, ASU and oxygen compressor;

[4] substitution of membrane and catalyst during power plant lifetime; average cost per year

**Table 6. Stream data for case B2 (see Figure 3 for stream numbers).**

| Stream | T (°C) | P (bar) | m (kg/s) | Molar fractions (%) | | | | | | | |
|---|---|---|---|---|---|---|---|---|---|---|---|
| | | | | Ar | $CH_4$ | CO | $CO_2$ | $H_2$ | $H_2O$ | $N_2$ | $O_2$ |
| 1 | 250 | 40 | 38.3 | NG, see text for composition | | | | | | | |
| 2 | 364.6 | 40.4 | 125.5 | | | | | | 100.0 | | |
| 3 | 600 | 38.8 | 163.8 | | 17.6 | 0.6 | 5.3 | 17.7 | 58.7 | 0.1 | |
| 4 | 600 | 34.8 | 146.7 | | 0.8 | 1.5 | 44.5 | 4.3 | 48.8 | 0.2 | |
| 5 | 256 | 34.1 | 7.6 | 3.7 | | | | | | 1.4 | 95.0 |
| 6 | 1012.1 | 32.91 | 154.7 | 0.2 | | | 45.8 | | 53.6 | 0.2 | 0.2 |
| 7 | 35 | 31.93 | 105.0 | 0.4 | | | 98.5 | | 0.2 | 0.5 | 0.5 |
| 8 | 30 | 110 | 104.9 | 0.3 | | | 98.7 | | | 0.5 | 0.5 |
| 9 | 436.1 | 19.82 | 169.8 | 1.0 | | | | | 0.9 | 77.3 | 20.7 |
| 10 | 484.3 | 19.8 | 151.7 | | | | | | 100.0 | | |
| 11 | 502.2 | 19.8 | 22.5 | | | | | | | 100.0 | |
| 12 | 850 | 19.7 | 361.0 | 0.2 | | | | 27.0 | 48.8 | 23.9 | |
| 13 | 450 | 19.6 | 361.0 | 0.2 | | | | 27.0 | 48.8 | 23.9 | |
| 14 | 15 | 1.01 | 553.3(×2) | 1.0 | | | | | 0.9 | 77.3 | 20.7 |
| 15 | 1409.5[a] | 16.54 | 474.3(×2) | 0.6 | | | | | 43.2 | 53.1 | 3.0 |
| 16 | 600 | 1.04 | 644.0(×2) | 0.7 | | | | | 33.4 | 58.8 | 7.2 |
| 17 | 80 | 1.01 | 1288.0 | 0.7 | | | | | 33.4 | 58.8 | 7.2 |

[a] stream temperature at the combustor exit

## EXERGY ANALYSIS RESULTS

Let's consider the exergy analysis of the proposed power plant, for two different cases: O64 and B2.

**Table 7. Exergy losses for cases O64, B2 and NGCC reference**

| | Exergy loss (% of exergy input) | | |
|---|---|---|---|
| | NGCC | O64 | B2 |
| Prereformer | | 2.00 | 2.18 |
| Membrane (combustion) | | 8.94 | 9.04 |
| Membrane (permeation) | | 0.87 | 0.83 |
| ASU+Oxy. compression | | 0.36 | 0.35 |
| Gas Turbine | 35.19 | 23.03 | 23.13 |
| HRSC | 6.34 | 4.23 | 4.40 |
| Combustion of retentate | | 1.24 | 1.23 |
| Heat Exchange | | 1.91 | 1.76 |
| Electrical losses | 1.50 | 1.20 | 1.14 |
| Various losses | | 0.36 | 0.19 |
| Stack losses | 2.95 | 5.93 | 6.89 |
| $CO_2$ compression | | 0.11 | 0.17 |
| **Total exergy losses** | **45.97** | **50.18** | **51.31** |
| **$CO_2$ captured** | | **3.67** | **3.68** |
| **Electricity** | **54.03** | **46.16** | **45.01** |

These cases have been selected to see the effect of pressure and S/C ratio on the plant exergy losses. For this analysis, obviously the $CO_2$ captured is not considered an exergy loss, but it is added to electricity as positive output. The reference power plant chosen for comparison is a conventional NGCC without $CO_2$ capture. Table 7 shows that case O64 adds an exergy loss of only 4% to that of the NGCC. Most of this difference, about 3%, is related to the presence of a high amount of steam, used as sweep gas, which ends up in the exhaust gases (see stack losses). Also the difference between O64 and B2 depends mainly on stack losses: the case O64 requires less sweep gas, due to the higher hydrogen partial pressure at the feed side. A lower S/C ratio decreases the exergy losses in pre-reformer and reformer. This analysis shows that the best way to improve the efficiency of this solution is to decrease the amount of steam used as a sweep gas.

## CONCLUSIONS

The integration of a membrane reactor with permeate side oxidation in a NGCC proves to be attractive from an efficiency point of view. Performance calculations indicate that the overall net electrical efficiency can be very high, above 48%, while using a large membrane surface area. With lower membrane surfaces, as suggested by economic considerations, the efficiency decreases, but still with good results, in particular considering that $CO_2$-emissions are close-to-zero. The influence of several parameters involved in the system, such as HRF, S/C ratio, membrane surface area, etc, were investigated.

The economic analysis shows that the membrane surface area has a large influence on the final investment costs. Usually is better to adopt relatively low membrane surface areas. The optimal case has an efficiency that is about 1.5 percentage points higher than conventional post combustion $CO_2$ capture technology, and a carbon capture ratio of 100% compared to 85%. From an economical point of view, the COE of the proposed solution is 30% higher than a NGCC without, and lower (6%) than conventional post combustion capture technology. The $CO_2$ avoidance costs are 31.2 €/t$CO_2$, which is over 35% lower than costs related to the conventional technology for carbon capture used as reference. These results indicate that this technology is a promising option for electricity production with low $CO_2$-emissions.

## ACKNOWLEDGMENTS

The authors gratefully acknowledge the financial support of the Dutch Ministry of Economic Affairs (EZ).

## REFERENCES

[1]Keller, A.E., 2003, *Steam reformer for methane with internal hydrogen separation and combustion*, Patent WO03031325.

[2]Moritsuka, H., 1999 *Hydrogen Decomposed Turbine Systems for Carbon Dioxide Recovery*, Elsevier Science Ltd., Kidlington, Oxford, pp. 563-568.

[3]Shu, J., et al., 1991, *Catalytic Palladium-based Membrane reactors: A Review*. The Canadian Journal of Chemical Engineering; 69, pp. 1036-1060

[4]Pex, P. P., et al., 2004, *Palladium alloy membranes for energy efficient membrane reactors,* Proc. Of the 8th international conference on Inorganic Membranes Cincinnati July 18-22, pp. 524-527

[5]Siriwardane, R.V., et al., 2003, *Characterization of ceramic-metal composite hydrogen separation membranes consisting of barium oxide, cerium oxide, yttrium oxide and palladium,* Applied surface science, 217, pp. 43-49

[6]Rusting, F. T., et al., *Sealing socket and method for sealing a socket into a tube*, Patent EP1257758, 2002.

[7]Horn, T., Glasser, R. P., Rackers, G., 2005, *Design, scale up and cost assessment of a membrane shift reactor, Carbon dioxide Capture for storage in deep geologic formation*, Vol1, Elsevier, pp 321-339

[8] Lozza, G., 1990, *Bottoming cycles for combined gas steam power plants: a theoretical estimation of steam turbine performance and cycle analysis*. Proceedings of ASME Cogen-Turbo, New Orleans, LA, USA pp.83-92

[9] Consonni, S., 1992 *Performance prediction of gas steam cycles for power generation*. PhD Thesis, MAE department n. 1983-T, Princeton University, Princeton, NJ, USA

[10] Chiesa, P., Consonni, S., Lozza, G., Macchi, E., 1993, *Predicting the ultimate performance of advanced power cycles based on very high temperature gas turbines engines*. ASME Paper 93-GT-223

[11] Macchi, E., Consonni, S., Lozza, G., Chiesa, P., 1995, *An assessment of the thermodynamic performance of mixed gas-steam cycles. Part A: Intercooled and steam injected cycles*. J Eng Gas Turb Power, 117, pp.489-498

[12] Chiesa, P., Macchi, E., 2002, T*hermodynamic analysis of different options to break 60% electric efficiency in combined cycle power plants*. ASME paper GT-2002-30663.

[13]Campanari, S., Macchi, E., 2002, *Thermodynamic analysis of advanced power cycles based upon solid oxide fuel cells, gas turbine and Rankine cycles*, ASME paper GT-2002-30663.

[14]Chiesa, P., Consonni, S., 1999, *Shift reactors and physical absorption for low-CO2 Emission IGCCs*, J Eng. Gas Turb. Power 121, 295 – 305.

[15]*Leading options for the capture of $CO_2$ emissions at power stations,* IEA report number PH3/14, February 2000

[16]Chiesa, P., Kreutz, T., Lozza, G., 2005 *$CO_2$ sequestration from IGCC power plants by means of metallic membranes*, Proc.of ASME TurboExpo , Reno-Tahoe, Nevada, USA

[17]Chiesa, P., Consonni, S., Kreutz, T., Williams, R., 2005 *Co-production of hydrogen, electricity and CO2 from coal with commercially ready technology. Part A.* Performance and emissions. International journal of hydrogen energy. 30 (7) pp.747-767

[18]Tosti, S., ENEA, personal communication

[19]Westerterp, K.R., Swaaij, W.P.M. van, and Beenackers A.A.C.M., *Chemical Reactor Design and Operation*, Wiley, 1984.

[20]*Improvement in power generation with post-combustion capture of $CO_2$* , IEA report number PH4/33, November 2004

[21]Kreutz, T., Williams, R., Consonni, S., Chiesa, P., 2005 *Co-production of hydrogen, electricity and CO2 from coal with commercially ready technology. Part B*. Economic analysis. International journal of hydrogen energy, 30(7), pp. 769-784

[22]*Dutch association of cost Engineers,* Prijzenboekje – 23 editie, NAP, 2003(in Dutch)